JGP Journal of General Physiology

ARTICLE

Differentially poised vesicles underlie fast and slow components of release at single synapses

Kris Blanchard*, Javier Zorrilla de San Martín*, Alain Marty, Isabel Llano, and Federico F. Trigo

In several types of central mammalian synapses, sustained presynaptic stimulation leads to a sequence of two components of synaptic vesicle release, reflecting the consecutive contributions of a fast-releasing pool (FRP) and of a slow-releasing pool (SRP). Previous work has shown that following common depletion by a strong stimulation, FRP and SRP recover with different kinetics. However, it has remained unclear whether any manipulation could lead to a selective enhancement of either FRP or SRP. To address this question, we have performed local presynaptic calcium uncaging in single presynaptic varicosities of cerebellar interneurons. These varicosities typically form "simple synapses" onto postsynaptic interneurons, involving several (one to six) docking/release sites within a single active zone. We find that strong uncaging laser pulses elicit two phases of release with time constants of ∼1 ms (FRP release) and ∼20 ms (SRP release). When uncaging was preceded by action potential–evoked vesicular release, the extent of SRP release was specifically enhanced. We interpret this effect as reflecting an increased likelihood of two-step release (docking then release) following the elimination of docked synaptic vesicles by action potential–evoked release. In contrast, a subthreshold laser-evoked calcium elevation in the presynaptic varicosity resulted in an enhancement of the FRP release. We interpret this latter effect as reflecting an increased probability of occupancy of docking sites following subthreshold calcium increase. In conclusion, both fast and slow components of release can be specifically enhanced by certain presynaptic manipulations. Our results have implications for the mechanism of docking site replenishment and the regulation of synaptic responses, in particular following activation of ionotropic presynaptic receptors.

Introduction

Prior to exocytosis, synaptic vesicles (SVs) move to the active zone, where they bind to a number of presynaptic proteins, and undergo various priming/docking steps (for review, see Südhof, 2012; Neher and Brose, 2018). These preparatory steps ensure not only efficient exocytotic responses to isolated action potential (AP) stimulations but also rapid replenishment of docking sites during AP trains (for review, see Hallermann and Silver, 2013; Pulido and Marty, 2017; Neher and Brose, 2018).

All SVs are not equally poised for exocytosis. At the calyx of Held, applying a step depolarizing voltage pulse to the presynaptic terminal leads to two successive components of SV release, with a fast time constant on the order of a few milliseconds and a slow time constant >10 ms (Sakaba and Neher, 2001). The corresponding fast-releasing pool (FRP) and slow-releasing pool (SRP) have roughly the same size (for review, see Neher and Sakaba, 2008). Following a common exhaustion by a prolonged presynaptic calcium transient, FRP and SRP recover with different kinetics. It has been suggested that FRP SVs are closer than SRP SVs to the voltage-gated calcium channels responsible for AP-induced calcium entry in the active zone ("positional priming"; Wadel et al., 2007) or else that FRP SVs have a special molecular configuration that allows them to fuse more readily than SRP SVs ("molecular priming"; Wölfel et al., 2007).

More recent findings indicate a sequential SRP/FRP SV recruitment on the way to exocytosis involving actin and myosin in the calyx of Held (Lee et al., 2012). Likewise, a sequential SV recruitment to a replacement site and an associated docking site has been proposed in cerebellar synapses (Miki et al., 2016). As in the calyx of Held, this two-step docking is sensitive to blockers of actin and myosin (Miki et al., 2016), suggesting that a docking release model involving two sequential states of differently poised SVs may be generally valid (for review, see Neher and Brose, 2018). In line with this suggestion, a rapid, very local movement of SVs toward their release site before

Université de Paris, SPPIN - Saints-Pères Paris Institute for the Neurosciences, Centre National de la Recherche Scientifique, UMR 8003, Paris, France.

*K. Blanchard and J. Zorrilla de San Martín contributed equally to this paper; Correspondence to Federico F. Trigo: federico.trigo@parisdescartes.fr; K. Blanchard's present address is Cell Physiology Laboratory, Faculty of Science, University of Chile, Santiago, Chile; J. Zorrilla de San Martín's present address is Institut du Cerveau et de la Moelle épinière, Centre National de la Recherche Scientifique, UMR 7225, Inserm U1127, Sorbonne Université Groupe Hospitalier Pitié Salpêtrière, Paris, France; F.F. Trigo's present address is Departamento de Neurofisiología Celular y Molecular, Instituto de Investigaciones Biológicas Clemente Estable, Montevideo, Uruguay.

exocytosis is suggested by recent studies using high-temporal-resolution electron microscopy (Chang et al., 2018; Kusick et al., 2018 *Preprint*). This final SV docking step depends on the cytosolic calcium concentration, in agreement with the known dependence of FRP recovery kinetics on calcium concentration (Hosoi et al., 2007). In spite of these advances, much remains to be learned about the generality of the SRP/FRP (or replacement SVs/docked SVs) distinction across synapses, as well as about the morphological and molecular underpinning of this distinction.

In the sequential SV recruitment model, the size of the FRP is limited by the total number of docking/release sites, which is thought to be fixed at a given active zone on a time scale of minutes (Neher and Sakaba, 2008; Neher and Brose, 2018). Recent results using electrophysiological recordings from cerebellar synapses containing a single active zone (called "simple synapses") indicate that at rest, the probability of occupancy of docking sites is <1, so that the FRP size is indeed significantly smaller than the number of docking/release sites (Trigo et al., 2012; Pulido et al., 2015; Miki et al., 2016). If this is so, then the FRP content may vary over time, perhaps as a function of basal calcium concentration, since SV replenishment is enhanced by calcium elevation (Neher and Sakaba, 2008). This could have important consequences concerning short-term synaptic plasticity (Miki et al., 2016; Neher and Brose, 2018).

In the present work, we use local calcium uncaging to show that simple GABAergic synapses of the cerebellum display two SV populations reminiscent of the SRP/FRP (or replacement SVs/docked SVs) distinction. Following synaptic release elicited by a conditioning train of presynaptic APs, we observe an increase of the slow component in response to a subsequent calcium uncaging stimulation. On the other hand, we find a selective enhancement of the fast component following a subthreshold calcium elevation. These results suggest that the FRP and SRP contributions to SV release may each be selectively enhanced depending on the previous synapse history.

Materials and methods

Slice preparation

Cerebellar slices were obtained as follows. Rats (11–17-d-old Sprague–Dawley) were killed by decapitation in accordance with institutional guidelines for ethical procedures (approval number A 750607). The cerebellar vermis was carefully dissected and placed in ice-cold bicarbonate-buffered solution (BBS; see composition below) that was constantly gassed with a mixture of 5% (volume/volume) CO_2 and 95% O_2. 200-µm-thick sagittal slices were cut with a vibroslicer (VT1200S; Leica) in ice-cold BBS and then placed in an incubating chamber at 34°C for 45 min to recover from the slicing damage. Thereafter, they were kept at room temperature until use. The slices were transferred to the recording chamber and used during a period of up to 8 h after isolation. The composition of the BBS for cutting, storing slices, and recording was (in mM) 115 NaCl, 2.5 KCl, 1.3 NaH_2PO_4, 26 $NaHCO_3$, 25 glucose, 5 Na-pyruvate, 2 $CaCl_2$, and 1 $MgCl_2$, with an osmolality of 300 mOsm/kg and pH 7.4 when gassed with 5% (volume/volume) CO_2 and 95% O_2.

Recording procedures

Molecular layer interneurons (MLIs) were selected based on their location in the molecular layer and the soma size, ranging from 6 to 8 µm. MLIs were voltage clamped with the whole-cell patch-clamp technique using a double EPC-10 USB amplifier (HEKA Elektronik). We used a high [Cl^-] in the postsynaptic intracellular solution (IS) in order to optimize the amplitude of postsynaptic currents (PSCs) and readily detect individual fusion events. The composition of the postsynaptic IS was as follows (in mM): 150 KCl, 1 EGTA, 10 HEPES, 0.1 $CaCl_2$, 4.6 $MgCl_2$, 4 Na_2ATP, 0.4 NaGTP, and 0.08 Alexa Fluor 488, with an osmolality of 300 mOsm/kg and pH 7.3. The composition of the presynaptic IS was 95 K-gluconate, 5.6 KCl, 50 HEPES, 0.5 $MgCl_2$, 4.2 $CaCl_2$, 5 Na_2ATP, 0.2 NaGTP, 5.2 KOH, 5 1-(2-nitro-4,5-dimethoxyphenyl)-N,N,N′,N′-tetrakis[(oxycarbonyl)methyl]-1,2-ethanediamine (DM-nitrophen; Synaptic Systems), 0.08 Alexa Fluor 594, and 10 γ-aminobutyric acid (GABA), with an osmolality of 300 mOsm/kg and pH 7.3. GABA was included in the IS to prevent rundown of the PSCs, as reported previously (Bouhours et al., 2011). Experiments were performed at room temperature (20–22°C), and the recording chamber was continuously perfused at a rate of 1–2 ml/min with gassed BBS. Nominal holding potentials were −60 mV for both presynaptic and postsynaptic neurons. After taking the calculated liquid junction potential of 13.8 mV and 1.4 mV into account, corrected holding potential values were −73.8 mV and −61.4 mV for the presynaptic and postsynaptic cells, respectively. Patch electrodes (micropipettes) were pulled from borosilicate glass to a tip resistance of ∼4.5 MΩ when filled with the postsynaptic IS and ∼7.0 MΩ when filled with the presynaptic IS. Series resistance was in the range of 10–35 MΩ and was not compensated. Cells were discarded when the series resistance value was >35 MΩ or if it varied >20% during recording. Recordings from both pre- and postsynaptic cells were acquired at a sampling rate of 50 kHz and low-pass filtered at 2.9 kHz. Approximately two thirds of the data were obtained from cells located in the proximal part of the molecular layer (basket cells), while another one third came from cells located in the outer molecular layer (stellate cells).

Finding a simple MLI–MLI synapse

To find a simple MLI–MLI synapse, we proceeded as described previously (Trigo et al., 2012). Starting with two neighboring MLIs located in the same horizontal plane, and taken as candidate pre- and postsynaptic partners, we first established a dual whole-cell patch clamp recording. Short depolarizing voltage steps of 1 ms to 0 mV were delivered to the potential presynaptic neuron to induce unclamped APs and test synaptic connectivity. For the group of experiments where vesicular release was tested only by using calcium uncaging (see Figs. 4 and 5), tetrodotoxin (0.2 µM final concentration) was included in the bath solution to minimize contamination from AP-dependent neurotransmitter release.

Photolysis of DM-nitrophen (Kaplan and Ellis-Davies, 1988) was done as previously described (Trigo et al., 2012; de San Martin et al., 2015). Briefly, 405-nm light from a diode laser (DeepStar; Omicron) was focused through a 63× Zeiss (1.0 NA) objective into a minimized (∼2 µm in diameter) laser spot;

alternatively, an Obis laser (Coherent) focused through a 60× Olympus (1.0 NA) objective was also used. As documented earlier, local laser stimulation resulted in calcium release in single small synapses containing a single presynaptic active zone and a single postsynaptic density of GABA receptors (Trigo et al., 2012). In the present work, we found that somatic synapses, unlike dendritic synapses, often contained several active zones. For this reason, results were restricted to dendritic synapses. Photolysis was obtained with 100–400-µs-duration laser pulses.

To choose the laser intensity, we used earlier results indicating that the entire set of docked SVs is released when using sufficient laser intensity and that under these conditions, most release events occur within 5 ms following the laser pulse (Trigo et al., 2012). To adjust laser intensity in individual experiments, we applied two consecutive laser pulses with a 30-ms interval (Fig. S1). Laser intensity was gradually increased until (1) most events occurred within 5 ms following the first laser pulse and (2) no <5-ms latency event was observed following the second laser pulse (Fig. S1). It proved important to make this adjustment for each experiment, because the effective laser intensity varied according to the depth of the recorded varicosity in the tissue.

Once the laser intensity was chosen, tests of presynaptic manipulations were repeated every minute. Responses were usually stable over a time period of ∼20 min (20 trials), after which the responsiveness of the synapse typically ran down and the experiment was interrupted. To minimize possible effects of run down, we systematically alternated control and test trials, and we always included the same number of control and test trials in individual experiments. The temporal sequence of applied protocols is represented by numbers in Fig. 4 A as an example. For the analysis of a given parameter (such as peak amplitude or latency), values in each condition were measured and averaged, so that in every case where gray points are displayed with a connecting line, the two connected points display mean results for the same synapse in control and test conditions.

Fluorescent images of pre- and postsynaptic MLIs and calcium imaging of the presynaptic MLI

Epifluorescence imaging was performed with two LEDs on a dual lamp-house controlled by an OptoLed (Cairn Research). The first LED excited the sample at 470 ± 40 nm and the second LED at 572 ± 35 nm. Emitted light (520 ± 40 nm and 630 ± 60 nm) was detected with an electron-multiplying charge-coupled device camera (Ixon; Andor). Filters were from Chroma Technology. For calcium imaging, the calcium indicator Oregon Green BAPTA-5N (OGB5) was included in the presynaptic IS at a final concentration of 500 µM and Oregon Green BAPTA-1 (OGB1) at a final concentration of 100 µM (both from Thermo Fisher Scientific). After an axonal varicosity was identified, it was positioned on the center of the camera chip by moving the preparation, and fluorescent images were acquired at a frame rate of 4.5 ms (218 Hz), in 2 × 2 binned pixels, with Andor Solis software. Fluorescence recordings presented in Figs. 3 and 4 correspond to averages of four or five interleaved (control and test protocols) trials and were acquired through the 60× Olympus (1.0 NA) objective. Unlike synaptic responses, calcium responses to laser pulses were stable over time, displaying no run down.

Analysis and statistics

Counting the release events

Individual release events were detected using TaroTools extensions (https://sites.google.com/site/tarotoolsregister/) implemented in Igor Pro (Wavemetrics). After a first automatic round, the selection of each event was visually confirmed before subsequent analysis. Latencies were measured as the time between the beginning of the laser pulse and the onset of individual synaptic currents (Fig. 1 B).

Analysis of calcium transients

The calcium transients presented in Figs. 3 and 4 were analyzed with custom-written routines running in Igor Pro as the fluorescence signal in relation to prestimulus values ($\Delta F/F_0$ presented in percentage).

Statistics

Data are presented as mean ± SEM. Whenever possible, we have compared mean values of a given parameter between control and test conditions in individual experiments, and then performed group analysis for several such experiments. In Figs. 2, 3, 4, and 5, we show the means for each experiment as gray dots linked by lines and the overall mean values across experiments in red, together with the corresponding ± SEM bars. Statistical differences between conditions were assessed with paired or unpaired Student's *t* test. The null hypothesis was rejected if $P < 0.05$. The cumulative latency histograms were adjusted by the sum of two exponentials with built-in routines in Python.

Cumulative histograms were fitted using least-squares method with the function

$$f(t) = Amp \times \left(1 - e^{\frac{-t+t_0}{\tau_f}}\right) + 1 - Amp \times \left(1 - e^{\frac{-t+t_0}{\tau_s}}\right),$$

where *Amp* is the relative amplitude, t_0 is the average minimal synaptic latency (t_0 = 0.6 in all cases), and τ_f and τ_s are the fast and slow time constants of the two exponential components, respectively.

Online supplemental material

Fig. S1 shows an example of a double laser experiment, which was the experiment performed in every recorded pair in order to choose the photolysis laser intensity. Fig. S2 shows an example of the fluorescent calcium transients recorded from one axonal varicosity with the high-affinity calcium indicator OGB1.

Results

Dual-component response to local calcium uncaging

Simple synapse recordings were performed as described previously (Trigo et al., 2012). In short, we performed dual patch-clamp recordings from neighboring MLIs, one of which was recorded with a solution containing the calcium cage DM-nitrophen. Dual recordings were selected such that the MLI recorded with the DM-nitrophen–containing solution (red

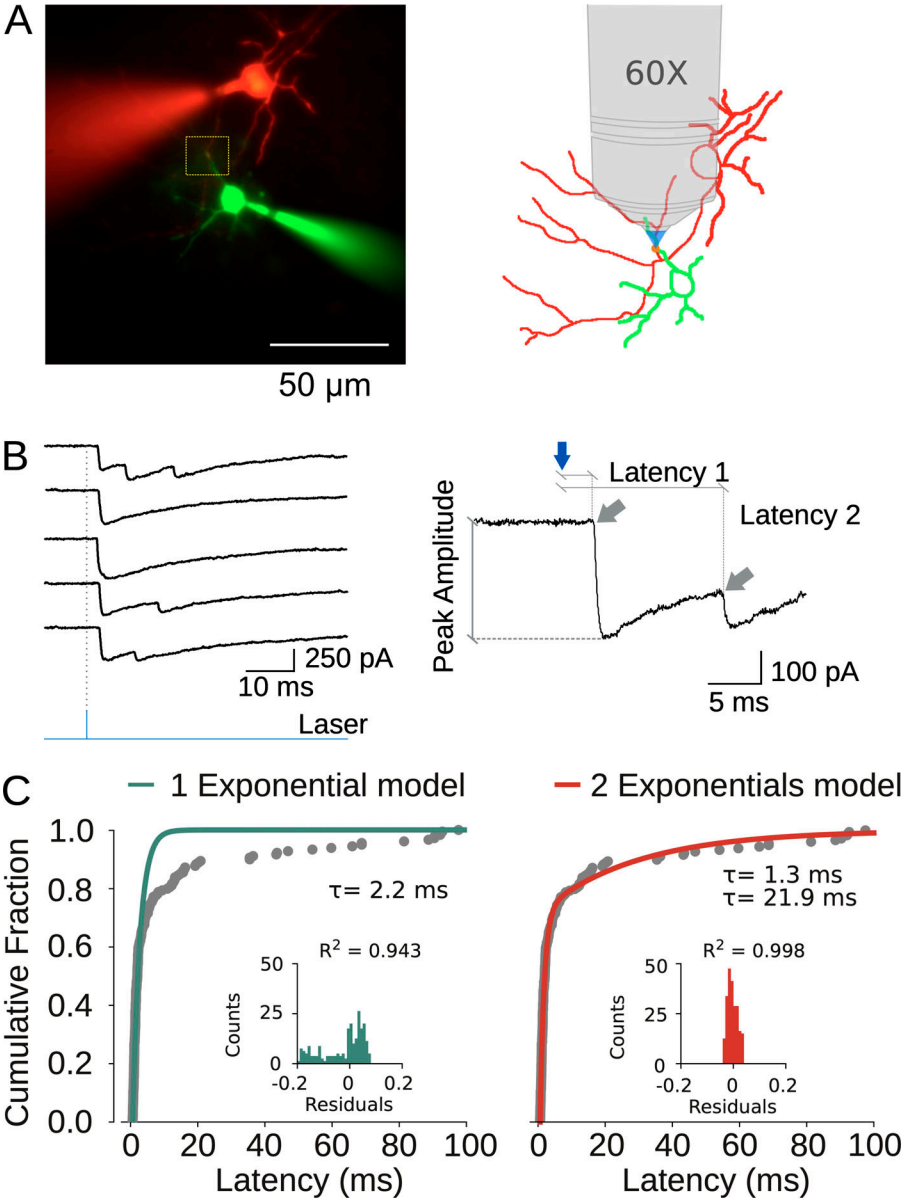

Figure 1. **Two-component response to local calcium uncaging at simple MLI–MLI synapses. (A)** Left: Dual-color image of presynaptic (red) and postsynaptic (green) MLIs with synaptic contact (dotted rectangle). Right: Reconstruction of pre- and postsynaptic cells (thick lines, dendrites; thin red line, presynaptic axon) together with positioning of laser spot illumination. **(B)** Left: Responses to individual laser stimulations (duration, 100 µs; power, 0.1 µJ; interstimulus period, 1 min). Right: Blowup of first response with measured latencies. Each latency likely corresponds to the release of one SV in this recording. Note the smaller amplitude of the second event, due to partial saturation of postsynaptic receptors. Note also that in some of the traces on the left (e.g., third trace), the exact number of released SVs is ambiguous because several SVs appear to be released almost simultaneously. The blue arrow corresponds to the laser stimulation; gray arrows indicate the beginning of the postsynaptic responses. **(C)** Group results showing latency distribution (236 events from 12 pairs). The distribution is well fit with a double exponential (right; amplitude of slow component, 27%). A lag of 0.6 ms was introduced between the laser pulse and the single or double exponential fits to account for the minimal latency of release responses.

solution in Fig. 1 A) was presynaptic to the other MLI (green solution in Fig. 1 A). Successful synaptic connection was assessed by applying APs to the presynaptic MLI and monitoring potential postsynaptic responses in the other MLI. Having obtained such a connection (with a success rate <10% of dual recordings), we followed the presynaptic axon and postsynaptic dendrites until a potential synaptic contact was identified (dotted rectangle in Fig. 1 A). Delivering a short (0.1–0.2-ms) and focused 405-nm laser light pulse to the contact site elicited synaptic responses (Fig. 1 B). These responses were abolished by micrometric lateral displacements of the laser beam, showing that they originate from the identified contact site (Trigo et al., 2012).

Previous work has shown that unitary MLI–MLI contacts involve a single presynaptic active zone and a single postsynaptic density (Auger and Marty, 1997; Nusser et al., 1997). Each of these synapses usually contains several docking/release sites (with numbers ranging between one and six among synapses), giving rise to multivesicular release in response to individual presynaptic APs (Auger et al., 1998; Pulido et al., 2015) and presynaptic calcium uncaging stimulations (Trigo et al., 2012). As the release of neurotransmitter from individual SVs activates a substantial proportion of postsynaptic receptors (Auger and Marty, 1997; Auger et al., 1998), multivesicular release is manifest as a succession of tiled current increments, where later events are smaller than earlier ones because of increasing receptor saturation (Fig. 1 B).

Under the conditions of Fig. 1, laser pulses elicit calcium rises that are long-lasting (>100 ms; Trigo et al., 2012; see data below) and homogeneous over the entire terminal. Approximately three quarters of the observed latencies occur 0.6–5 ms following the laser pulse, while approximately one quarter occur over the subsequent 5–100-ms period (Fig. 1 C). Overall, a single exponential offers a poor fit to the cumulative latency distribution (Fig. 1 C, left), whereas a double exponential is a more accurate description of the observed distribution (Fig. 1 C, right; fast time constant, 1.3 ms; slow time constant, 21.9 ms; percentage of slow

component, 27%). The widely different time constants suggest two categories of SVs with different release properties, similar to the FRP and SRP of the calyx of Held and other synapses (Wölfel et al., 2007; Hallermann et al., 2003, 2010). More specifically, it is plausible that the fast component reflects the immediate release of docked SVs, belonging to the FRP, while the second component reflects a two-step release event (Miki et al., 2018), where a SV initially in the SRP would undergo a sequence of docking followed by release. Alternatively, the initial burst of release could correspond to the emptying of the readily releasable pool (RRP; possibly containing both FRP and SRP components, which would then be unresolved), while the second component would reflect late release events following replenishment of the RRP from the recycling pool (Wadel et al., 2007; Sakaba, 2008).

A presynaptic AP train evoked before local calcium uncaging modifies the proportion of fast and slow release

We next attempted to test the sensitivities of the <5-ms latency component ("fast" component) and the >5-ms latency component ("slow" component) to various experimental manipulations, with the hope of obtaining differential responses to these manipulations. The first manipulation consisted of a short conditioning train of five presynaptic APs. As illustrated in Fig. 2, the effect of the AP train on the response to a subsequent test laser pulse depended on whether the train resulted in failures (Fig. 2 A, left; as already shown, AP propagation is highly reliable in MLIs, with no conduction failures; Forti et al., 2000) or a synaptic response (Fig. 2 A, right). In the second case, the fast-component response to the laser pulse was typically reduced in amplitude, while the frequency of slow release events was enhanced, compared with trials with failures (Fig. 2 A).

Group analysis confirmed that the average peak response to local calcium uncaging, which always took place within 5 ms following the laser pulse, was reduced from 205 ± 43 pA to 167 ± 39 pA by the preceding AP-induced synaptic release (mean percentage reduction in individual experiments, 74 ± 13%, n = 7; paired t test, P = 0.016; Fig. 2 B). The inhibition of the fast component apparent in Fig. 2 B is consistent with earlier results in the calyx of Held, showing a reduction of the fast component of laser-induced release by previous synaptic release (Schneggenburger and Neher, 2000). As in this previous work, we interpret the inhibition of the fast component as reflecting a reduction in the number of SVs immediately available for release, that is, a reduction in the proportion of docking sites that are occupied by SVs. To assess potential effects of prior synaptic release on the relative weight of fast and slow component, we compared cumulative latency histograms in trials without and with responses to the AP trains, as well as in trials without the trains. The results show a marked increase in the proportion of slow events, growing from 22 ± 1.4% in trials without responses to AP trains (gray data points and associated biexponential fit) and 29 ± 0.3% in trials without AP trains (red; same data as in Fig. 1) to 57 ± 0.5% in trials with responses to AP trains (blue; fits were obtained with a common fast time constant of 1.2 ms and a common slow time constant of 28 ms; one-way ANOVA, $F_{(2,32)}$ = 5,997, P < 0.001; Fig. 2 C). Consistent with the cumulative latency histograms results of Fig. 2 C, paired comparison revealed an increase in mean latencies following successful responses to the conditioning train (from 5.7 ± 1.6 ms to 12.7 ± 2.0 ms; P = 0.02, paired t test; Fig. 2 D). These results suggest that successful conditioning APs alter the fast/slow proportion of the subsequent test responses in favor of the slow component.

In a further attempt to quantify this effect, we compared counts of events that could be distinguished in the fast and slow component, with and without a response to the conditioning AP train. We found no change in the counts of fast events (trains with failures, 0.98 ± 0.09 SVs; trains with PSCs, 0.98 ± 0.14 SVs; P = 0.89; Fig. 2 E, left) and an increase of slow-event counts for successful conditioning AP trains (trains with failures, 0.33 ± 0.12 SVs; trains with PSCs, 0.87 ± 0.4 SVs; P = 0.03; Fig. 2 E, right). When interpreting the fast-component results, it has to be remembered that unresolved multivesicular release tends to underestimate the numbers of this component (Trigo et al., 2012). Since the release number was close to 1 on average, whereas MLI synapses display multivesicular release (Trigo et al., 2012; Pulido et al., 2015), it appears that many release events of the fast component failed to be reported. Therefore, the apparent lack of effect of successful conditioning AP trains on fast-component counts may be due to underreporting of multivesicular events, and it is compatible with the inhibition seen on peak amplitudes (Fig. 2 B). Overall, the results indicate that synaptic release during conditioning APs decreases the fast component and increases the slow component.

As illustrated in Fig. 2 C, the size of the slow component was similar for trials without AP trains and for those with AP trains but without synaptic responses to these trains. In line with this result, the mean average latency was similar without conditioning APs (6.7 ± 1.5 ms) and with unsuccessful conditioning APs (5.9 ± 1.5 ms, P = 0.39). These results suggest that the effects of an AP train on the uncaging response are not mediated by a modification of the uncaging-induced calcium signal, since AP trains that failed to elicit a synaptic response did not modify the uncaging response. To test this point directly, we performed imaging experiments where the local calcium concentration was monitored in single varicosities with the low-affinity dye OGB5 (K_d ≈30 µM; Faas et al., 2005). When applying the AP trains, no calcium response was registered (yellow trace, Fig. 3 A). This indicated that the time- and space-averaged calcium rise was small compared with the dye dissociation constant. Presumably, calcium transients resulting from the activation of voltage-gated calcium channels were severely restricted in time and space (Llinás et al., 1992; Schneggenburger and Neher, 2000) and were therefore not visible at the spatiotemporal resolution of our measurements. By contrast, calcium transients elicited by uncaging were well resolved (responses to laser pulse in Fig. 3 A). These transients had a mean amplitude of 59.9 ± 9.5% in control conditions and of 64.0 ± 8.5% following conditioning APs (P = 0.15, paired t test, n = 10). The decay time constant had a mean of 126 ± 34 ms in control conditions and 139 ± 39 ms following conditioning APs (P = 0.16, paired t test, n = 10). These results indicate that conditioning APs did not modify the amplitude or decay time constant of the uncaging calcium transients (Fig. 3 B).

In conclusion, our results indicate that conditioning APs do not alter the uncaging calcium transient or the release

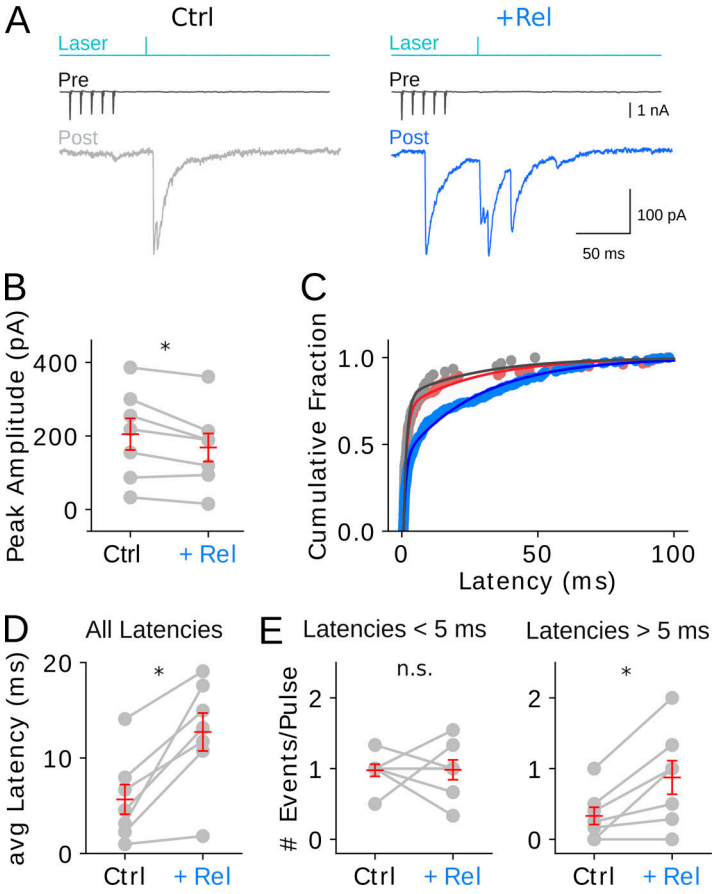

Figure 2. **Selective enhancement of slow component with conditioning AP train. (A)** Left: Fast response to laser stimulation following a train of five presynaptic APs without any synaptic response (Ctrl). Right: Following another five-AP train, a synaptic response is obtained (+Rel). The fast response is then reduced in amplitude and is followed by several release events with latencies >5 ms (slow response). **(B)** Average fast response amplitudes are reduced in six out of seven experiments following AP-induced synaptic responses compared with AP-induced failures, with an average amplitude reduction of 26%. **(C)** Cumulative latency distributions indicate a larger slow component following AP-induced synaptic responses (57%; blue) compared with trials where APs led to synaptic failures (21%; gray) or trials without conditioning AP (29%; brown, same data as in Fig. 1C; all fits were constrained to a common fast time constant value of 1.2 ms and a common slow time constant value of 28 ms, based on the blue data points). **(D)** Paired comparison shows larger average latencies for trials displaying synaptic responses compared with trials where APs led to failures (n = 7 experiments). **(E)** Paired comparison shows similar numbers of short release events (<5-ms latencies, left) and larger numbers of slow release events (>5-ms latencies, right) for trials displaying synaptic responses compared with trials where APs led to failures (n = 7 experiments). Gray points show averages in Ctrl and +Rel conditions in B, D, and E, while average values across experiments and associated ± SEM bars are in red. n.s., not significant *, P < 0.05, paired t test.

probability of available SVs and that they influence the response to a subsequent laser pulse only inasmuch that they elicit release themselves.

As mentioned earlier, the decrease of the fast component likely reflects a decrease in the RRP following AP-induced synaptic release. The finding that this leads to an increase of the slow component puts constraints on the mechanistic interpretation of fast and slow components. If the fast component was reflecting RRP release while the slow component was reflecting RRP replenishment, as suggested for synapses between MLIs and Purkinje cells (Sakaba, 2008), then decreasing the RRP with conditioning AP stimulations would decrease the fast component but would not alter the slow component. If, however, the fast component corresponds to only part of the RRP (docked SVs, or FRP SVs) while the slow component corresponds to another part of the RRP (replacement SVs, of SRP SVs), then it is conceivable that removing SVs from the first pool would facilitate release from the second pool, as further discussed below. Therefore, the results of Fig. 1 favor an interpretation of the fast and slow components as reflecting two kinds of SVs that belong to the RRP but are differently poised for exocytosis (FRP/SRP or docked/replacement SVs).

Selective enhancement of the fast component with subthreshold calcium elevation

We next asked whether a subthreshold global calcium transient would be able to change the size of the fast vesicle component. The experimental protocol is shown in Fig. 4 A. Like above, control runs consisted of strong single laser pulses releasing a large fraction of available SVs (Fig. 4 A, black traces). Compared with the experiments described so far, the amplitude of the laser pulse was somewhat lower. Accordingly, the mean first latency was 1.8 ± 0.1 ms, compared with 1.0 ± 0.1 ms in the previous series of experiments (see Materials and methods, procedure to adjust laser intensity; and Fig. S1). As will be explained below, we used this range of latencies in order to be able to analyze latencies of individual SV events at least in some experiments. In test runs, a series of five smaller laser pulses (with 10-fold smaller amplitude and interpulse intervals of 100 ms) preceded the test pulse, leaving an interval of 100–200 ms between the end of the conditioning pulses and the test pulse. Contrary to the situation of Fig. 2, the smaller pulses did not elicit any detectable synaptic response (Fig. 4 A, yellow traces). Nevertheless, they altered the response to the test pulse. As illustrated in the example shown, the average peak amplitude was increased by the presence of laser prepulses (yellow and black traces in Fig. 4 B). Group results for the 100-ms versus 200-ms interval did not reveal any difference between the two datasets, and they were therefore pooled together. The pooled results confirmed a significant increase of the peak amplitude associated with prepulses, which grew from 156 pA to 180 pA (a 15% increase; P = 0.01, n = 17; Fig. 4 C, left). By contrast, the number of release events per trial belonging to the slow component did not change (control, 0.285 ± 0.076; with prepulses, 0.282 ± 0.068; P = 0.81; paired t test).

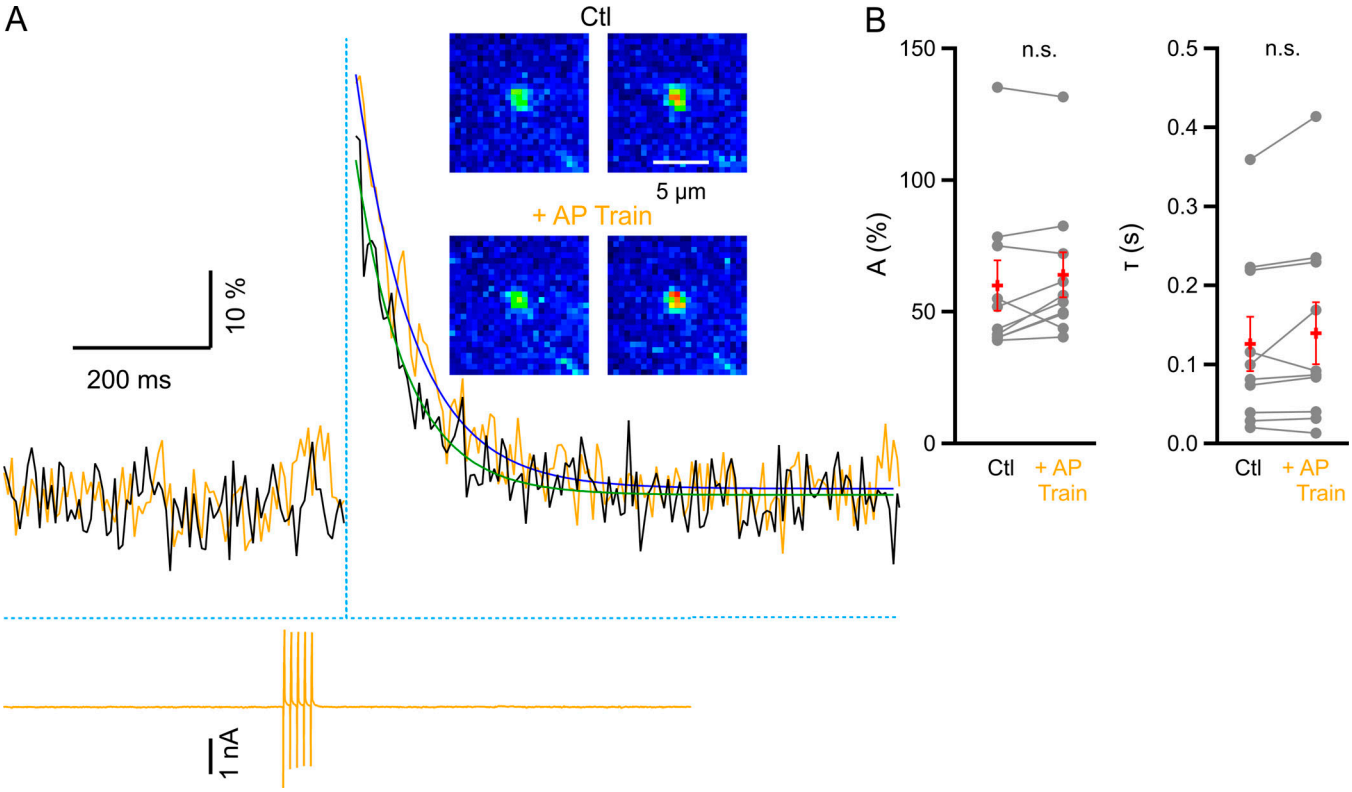

Figure 3. **Conditioning AP train does not alter calcium response to subsequent laser stimulation. (A)** Inset: Calcium imaging of presynaptic varicosity (0.5 mM OGB5 in recording pipette) before (left) and after (right) laser stimulation, without (top) or with (bottom) conditioning AP train. Main plot: Traces of OGB5 fluorescence signal in response to laser pulse (blue), without (black) or with (yellow) conditioning AP train (yellow trace). **(B)** Group results (n = 10; gray, individual cells; red, averages ± SEM) showing no effect of conditioning AP train on laser-evoked calcium transient peak amplitude (left) or time constant of decay (right; see exemplar exponential fits in A). n.s., not significant.

Paired analysis revealed a significant shortening of first latencies with prepulses (Fig. 4 C, right), in line with the potentiating effect observed on peak amplitudes. To gain insight into the duration of the potentiation, we repeated the same experiments with a 2-s interval between the end of the prepulses and the test pulse. We then found no effect on either peak amplitudes (control, 215 ± 44 pA; with prepulses, 197 ± 36 pA) or first latencies (control, 1.75 ± 0.19 ms; with prepulses, 1.75 ± 0.29 ms; P > 0.05 for both comparisons; paired t test, n = 9; Fig. 4 D). Therefore, potentiation only occurs for relatively short intervals between conditioning and test pulses.

Next, we examined possible effects of prepulses on the basal calcium concentration as well as on the calcium transient induced by the test pulse (Fig. 4 E). When using as before the indicator OGB5, the fluorescence signal associated with prepulses was very weak and was largely buried in the recording noise, indicating that the associated calcium increase was in the submicromolar range (Fig. 4 E, compare yellow and black traces before the test laser pulse). Later in the traces, responses to the test pulse were very similar with and without prepulses (Fig. 4 E). Group results did not reveal any significant change in the amplitude or time constant of decay of the response to the test pulse when it was preceded by prepulses (amplitude without prepulses, 103.3 ± 12.8%; amplitude with prepulses, 114.7 ± 14.9%; time constant of decay without prepulses, 116.8 ± 20.8 ms; time constant of decay with prepulses, 146.4 ± 23.8 ms; P > 0.05 for both comparisons, paired t test, n = 9; Fig. 4 F). We also performed the same type of recordings from three varicosities with the high affinity calcium indicator OGB1 (Fig. S2); these indicate that the maximum calcium concentration reached at the end of the subthreshold laser uncaging pulses is around the K_d of the dye, ~170 nM. These results indicate that the potentiating effect of prepulses is not due to an increased basal calcium concentration at the time of the test pulse or to an increase in the amplitude of the calcium transient induced by the test laser pulse.

Enhanced release probability following subthreshold calcium elevation

As mentioned above, in many experiments, unresolved multivesicular release prevented us from obtaining reliable counts of the fast component of release. Nevertheless, in seven experiments with subthreshold laser pulses, time separation between events was sufficient to allow for counting of individual release events. In the example shown in Fig. 5 A, the maximum number of released SVs was two, suggesting that the synapse had two docking sites (Trigo et al., 2012). The distribution of trials with zero, one, or two SVs could be fit with a binomial distribution, suggesting two independent docking sites, each having a release probability, P, of 0.40 (Fig. 5 A, bottom). In intercalated trials

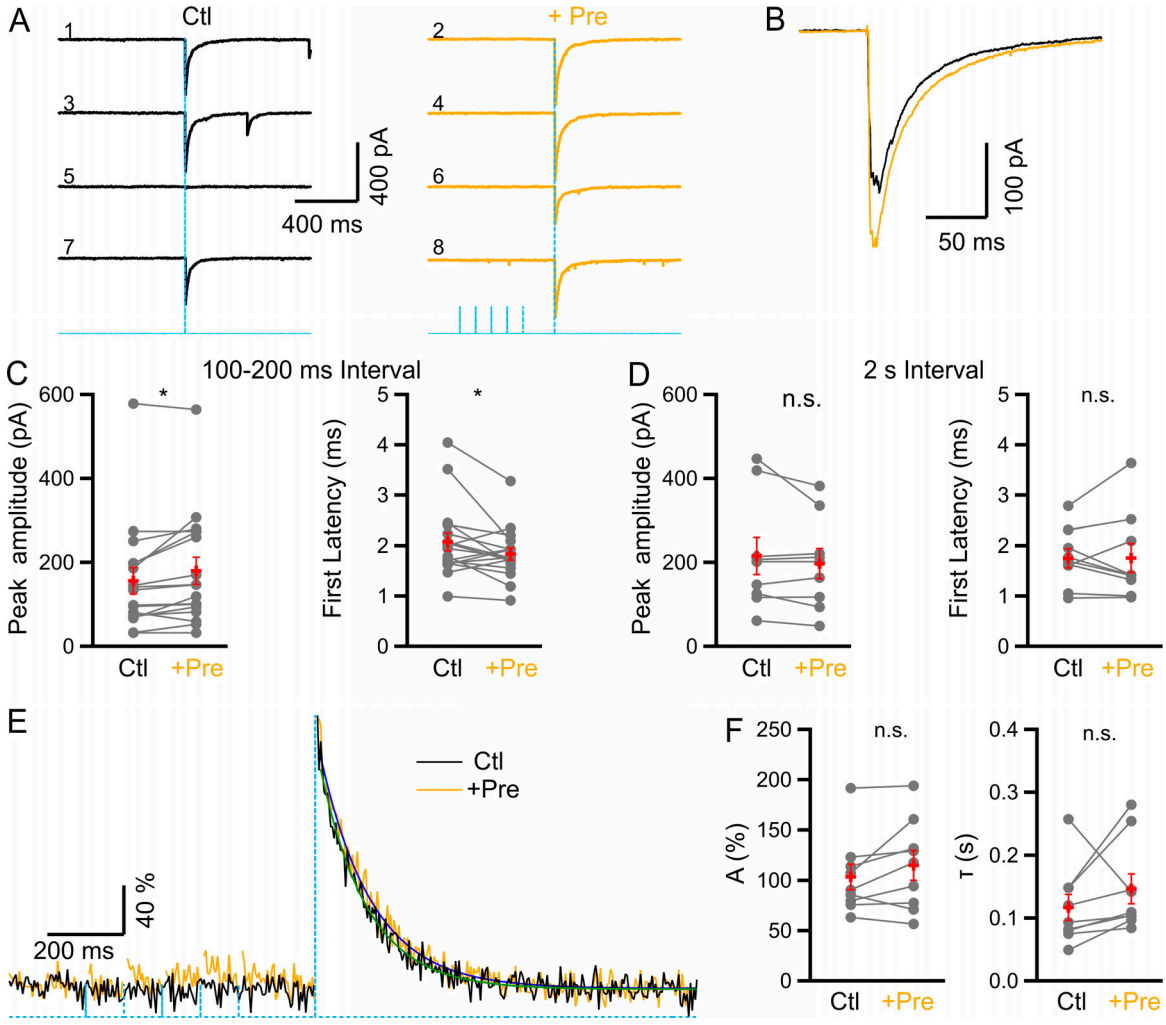

Figure 4. **Potentiation of fast release component following subthreshold calcium uncaging. (A)** Exemplar traces (presented in chronological sequence, from left to right and from top to bottom) showing responses to large test laser stimulations in either the absence (left, black traces) or the presence (right, yellow traces) of a series of five small-amplitude laser prepulses (bottom, blue traces). **(B)** Average traces without (black) and with (yellow) prepulses from the same experiment as in A. **(C)** Group results (gray, averages across trials for individual experiments; red, averages ± SEM across experiments) reveal a significant amplitude potentiation following prepulses (left) as well as a significant shortening of first latencies (right) when using prepulses (+Pre) compared with control (delay to test pulse, 100 or 200 ms). *, P < 0.05, paired *t* test. **(D)** Increasing the delay from 100–200 ms to 2 s abolishes the potentiation of the peak amplitude (left) as well as the shortening of the first latency (right). n.s., not significant **(E)** Exemplar calcium imaging traces from a single presynaptic varicosity in response to a test laser flash alone (black) or preceded by a train of five small-amplitude flashes (yellow), with superimposed exponential fits of test laser-induced response. **(F)** Group results showing no effect of preceding laser pulses on peak amplitude (left) or time constant of decay (right) of test flash response (*n* = 9 varicosities; gray, individual experiments; red, averages ± SEM).

with prepulses, the maximum number of SVs was again two, suggesting that the same number of docking sites applied to both control and test trials. In test trials, however, the distribution was shifted toward larger numbers, and the release probability rose to P = 0.55 (Fig. 5 B). Similar results were found in the other six recordings where the same type of analysis could be performed. Group analysis indicated a significant increase of P from 0.40 ± 0.04 in control to 0.52 ± 0.05 with prepulses (paired *t* test, P < 0.01; *n* = 7; Fig. 5 C). These numbers indicate a mean ratio of 1.3 between control and test P values; that is, a value larger than the corresponding peak amplitude ratio (1.15). This difference probably arises because in peak amplitude measurements, partial receptor saturation attenuates multivesicular synaptic responses, leading to a sublinear relation between SV number and peak amplitude (Auger et al., 1998).

Next, we took advantage of the detection of individual SV counts to compare means of all SV release latencies with and without prepulses. As shown in Fig. 5 D, means of all fast component (<5 ms) latencies were not affected by prepulses, whereas means of first latencies decrease with prepulses (Fig. 4 C, right). It has long been recognized that if the time course of the instantaneous release probability as a function of time does not change during synaptic potentiation, then an overall increase in release probability is associated with a shortening of the first latency without any change in the mean latency (Barrett and Stevens, 1972). In the present case, this is the prediction of a situation where prepulses would increase the FRP size (the

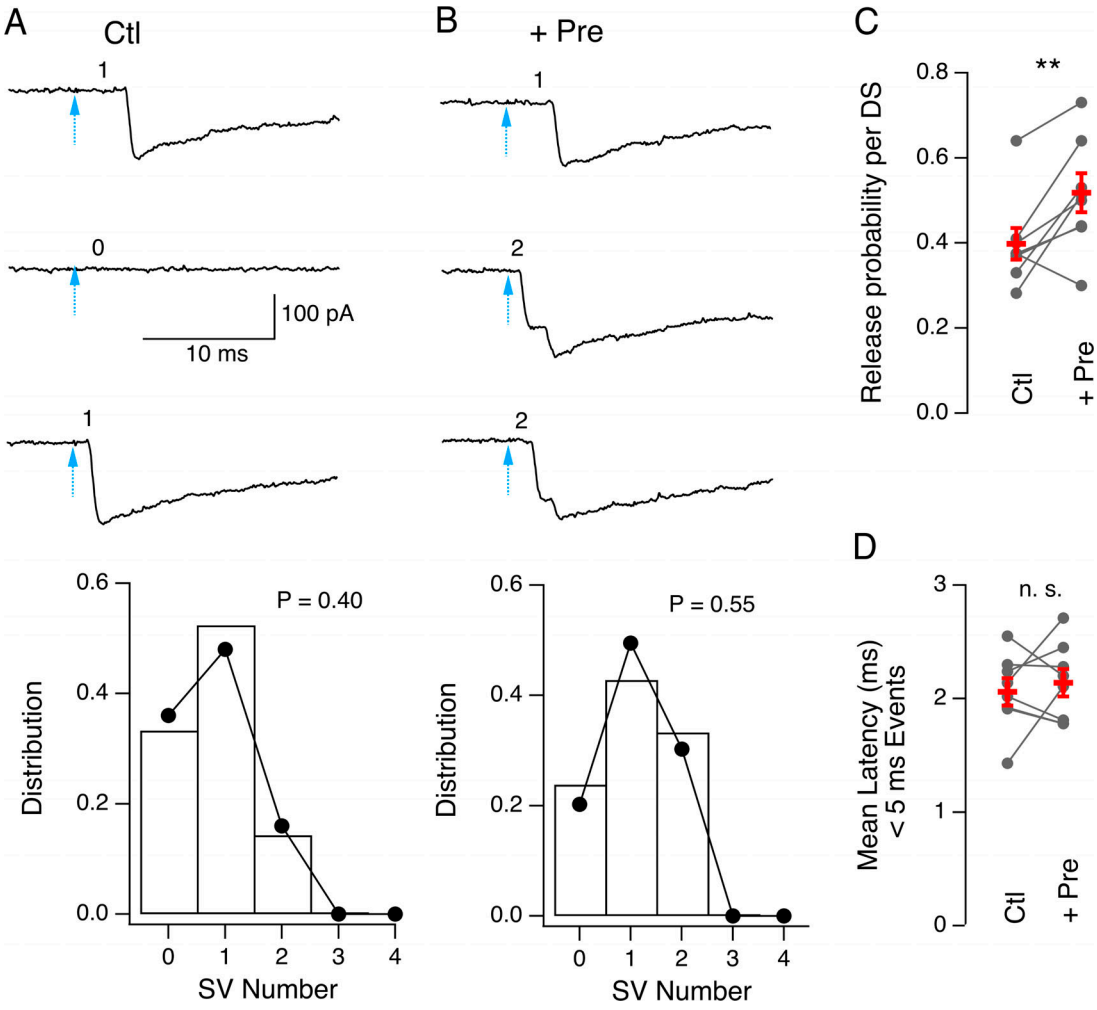

Figure 5. **Enhancement of release probability following subthreshold calcium uncaging. (A)** Top: Sample traces showing examples of failure (middle trace) and single SV responses (top and bottom traces) to test laser stimulation (arrows). Bottom: Experimental distribution of SV release numbers (bar graph) and superimposed fit with a binomial distribution (dots) assuming two independent docking sites. **(B)** Top: Intercalated trials including prepulses from the same experiment display more frequent examples of dual SV responses (second and third traces). Bottom: Binomial analysis of these data indicates an increase of the release probability per docking site from P = 0.40 in control to P = 0.55 with prepulses. **(C)** Group analysis from seven pairs showing a significant increase in P with prepulses. **, P < 0.01, paired *t* test. **(D)** Prepulses do not alter the means calculated for all latencies of the fast component (<5 ms). DS, docking site; n.s., not significant.

number of docked SVs) without changing the release probability of docked SVs (which is probably close to 1, both without prepulses and with prepulses).

Altogether, the analysis of individual SV release events points at the release probability P as the parameter responsible for potentiation. In general, P is the product of the probability of occupancy of docking sites, P_{occ}, with the probability of release of docked SVs, P_{rel} (Vere-Jones, 1966). Under the conditions of strong calcium uncaging, P_{rel} is close to 1, so that P is close to P_{occ} (Trigo et al., 2012). Therefore, our results suggest that the potentiation mainly represents an increase in the probability of occupancy of docking sites.

Discussion

In this work, we show two components of calcium-induced SV release at MLI–MLI synapses: a fast component with a time constant near 1 ms and a slow component with a time constant near 20 ms. We further show that preceding AP-induced synaptic release reduces the size of the fast component and increases the size of the slow component. By contrast, we find that a conditioning global calcium elevation in the subthreshold range increases the size of the fast component. As we shall see, these results have implications on the mechanisms of SV recruitment at this synapse.

Tentative identification of the fast/slow components as FRP/SRP and as docked/replacement SVs

Our previous work based on variance-mean analysis of summed SV counts during trains suggests that at MLI–MLI synapses, as in PF–MLI (parallel fibers to MLI) synapses, each release site is associated with up to two SVs, respectively bound to a docking site and a replacement site (Miki et al., 2016; Fig. 6). Incoming SVs first bind to the replacement site and then to the associated

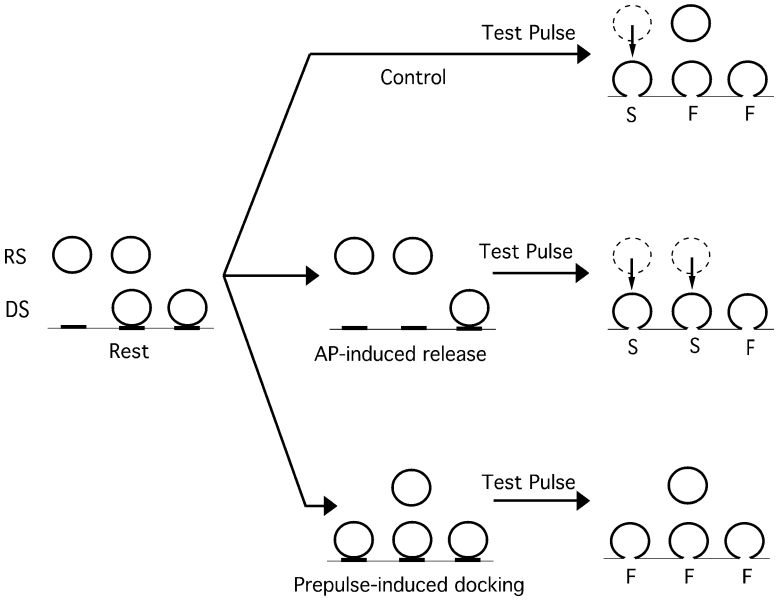

Figure 6. **Interpreting changes in the proportion of fast and slow components of laser-induced responses.** Schematic representation of an MLI active zone possessing three docking sites (DSs), two of which are occupied at rest, and three associated replacement sites (RSs), two of which are occupied at rest. Under control conditions, docked SVs give rise to fast release (F), whereas replacement SVs give rise to slow release (S), in a two-step process including docking then release (vertical arrows). Following AP-induced release, some docking sites are freed, so that the proportion of slow release is increased. By contrast, following prepulse-induced docking, the proportion of fast release is increased.

docking site before undergoing exocytosis (Miki et al., 2016; Pulido and Marty, 2018). In view of this earlier work, we tentatively identify the fast and slow components as reflecting the release of docked SVs and of replacement SVs respectively. To explain the difference in release kinetics, we suggest that docked SVs are directly released within a few milliseconds, whereas replacement SVs must first move to the docking site before being released, following a process earlier described as "two-step release" (Miki et al., 2018). It is plausible that docked SVs and replacement SVs respectively represent the FRP and SRP described at the calyx of Held (Neher and Sakaba, 2008), so we also tentatively associate the fast and slow components respectively to FRP and SRP (Fig. 6).

Effects of previous AP-induced release

Presynaptic APs produce quick calcium rises that do not elicit two-step release under normal conditions. Accordingly, AP-induced release only concerns the FRP (docked SVs; Sakaba, 2006; Miki et al., 2018). In our work, we interpret the effects of previous AP-induced release on subsequent responses to strong laser pulses as follows. Clearly, these effects depend on conditioning APs effectively inducing SV release, indicating that they are due to a decrease in the number of docked SVs. As the waiting time between conditioning APs and test laser pulse (typically 50 ms) is short compared with the kinetics of docking at MLI–MLI synapses (Pulido et al., 2015), the loss of docked SVs has not yet been compensated fully by docking of replacement SVs by the time of arrival of the test laser pulse. This readily explains the decreased fast component response associated with successful conditioning AP trains. On the other hand, by emptying docking sites, these trains create new options for two-step release of replacement SVs following the laser test pulse (Fig. 6, second row). Thus, a reduction of the number of docked SVs gives a plausible explanation both for the reduction of the fast component and for the augmentation of the slow component.

While successful AP-induced SV release reduces the number of docked SVs, it should not increase the number of replacement SVs (Fig. 6, second row). It may seem paradoxical that the slow component should increase if the number of replacement SVs does not increase and may in fact even slightly decrease as some replacement SVs move toward the docking site following release of an associated docked SV. However, it has been argued that a "refractory period" follows SV release at each docking site (Hosoi et al., 2009). Provided that such a refractory period lasts for >20 ms (the time constant of the slow component), it would prevent two-step release in sites possessing both a docked SV and a replacement SV at the time of the test pulse. On the other hand, if the refractory period is shorter than the delay between the end of the AP train and the test laser pulse (50 ms), it does not prevent two-step release in response to the test pulse at a site that has been freed by the APs. A previous estimate of the refractory period based on modeling at PF–MLI synapses (40 ms) is in line with these constraints (Miki et al., 2018). Thus, the increased slow component does not reflect an increased number of replacement SVs but rather an increased likelihood of two-step release following the freeing of docking sites.

Effect of previous subthreshold calcium elevation

It has previously been shown that a subthreshold presynaptic calcium elevation leads to a potentiation of subsequent synaptic current responses to APs (Bouhours et al., 2011; Christie et al., 2011). Our results are consistent with these earlier findings, and in addition, they suggest a specific mechanism by which release is increased, namely an increase in docking site occupancy. To have such an effect, two conditions must be met. First, docking sites should not be fully occupied at rest. Our previous work provides evidence in favor of this, with estimates of docking site occupancy ranging from 0.45 (Pulido et al., 2015) to 0.7 (Trigo et al., 2012). Our present estimate of 0.4 is compatible with this earlier work. The second condition is that the presynaptic calcium elevation leads to a shift of the equilibrium between the

replacement site and docking site in favor of docking. This second condition is in line with much experimental evidence in many systems, indicating that docking site replenishment is favored by calcium elevation (Neher and Sakaba, 2008), as well as with recent additional evidence based on time resolved electron microscopy (Chang et al., 2018; Kusick et al., 2018 *Preprint*). Our results suggest that, following calcium elevation, increased docking lasts for ≥200 ms and at most for 2 s. Therefore, increased docking takes place on the time window of short-term synaptic plasticity. Increased docking presumably occurs in MLIs following subthreshold somatic depolarization due to passive spread of depolarization to presynaptic terminals (Bouhours et al., 2011; Christie et al., 2011). In addition, many physiologically relevant manipulations are known to increase presynaptic calcium and may therefore lead to increased docking. At the calyx of Held, activation of presynaptic GABA receptors or glycine receptors leads to elevation of the bulk presynaptic calcium concentration, thus increasing evoked glutamate release (Turecek and Trussell, 2002; Awatramani et al., 2005). In MLIs, activation of presynaptic AMPA (α-amino-3-hydroxy-5-methyl-4-isoxazolepropionic acid) receptors (Rossi et al., 2008) or NMDA receptors (Rossi et al., 2012) leads to an increase in presynaptic calcium concentration and increased GABA release. Likewise, activation of presynaptic $GABA_A$ receptors depolarizes terminals and increases GABA release in MLI axons (Trigo et al., 2007; de San Martin et al., 2015) and Purkinje cell axons (Zorrilla de San Martín et al., 2017). All of these effects are possibly mediated through increased SV docking. Given the large number of similar examples in numerous brain neuron preparations, the potential functional importance of calcium-driven increased docking can hardly be overrated.

Acknowledgments

Richard W. Aldrich served as guest editor.

We thank Van Tran for useful comments on the manuscript.

This work was supported by the Agence Nationale de la Recherche (Jeune Chercheur, grant ANR-17-CE16-0011 to F.F. Trigo), the European Research Council ("SingleSite", advanced grant 294509, to A. Marty), a Comisión Nacional de Investigación Científica y Tecnológica grant (CONICYT PFCHA/DOCTORADO NACIONAL/2014 – 21140748 to K. Blanchard), and by a Fondo Nacional de Desarrollo Científico y Tecnológico grant (Fondecyt; grant 1140520, to Juan Bacigalupo).

The authors declare no competing financial interests.

Author contributions: K. Blanchard, J. Zorrilla de San Martín, A. Marty, I. Llano, and F.F. Trigo designed experiments. K. Blanchard, J. Zorrilla de San Martín, and F.F. Trigo performed electrophysiological experiments on simple synapses. I. Llano and F.R. Trigo performed imaging experiments on presynaptic varicosities. All authors participated in data analysis and writing the manuscript.

Submitted: 30 October 2019
Accepted: 12 March 2020

References

Auger, C., and A. Marty. 1997. Heterogeneity of functional synaptic parameters among single release sites. *Neuron.* 19:139–150. https://doi.org/10.1016/S0896-6273(00)80354-2

Auger, C., S. Kondo, and A. Marty. 1998. Multivesicular release at single functional synaptic sites in cerebellar stellate and basket cells. *J. Neurosci.* 18:4532–4547. https://doi.org/10.1523/JNEUROSCI.18-12-04532.1998

Awatramani, G.B., G.D. Price, and L.O. Trussell. 2005. Modulation of transmitter release by presynaptic resting potential and background calcium levels. *Neuron.* 48:109–121. https://doi.org/10.1016/j.neuron.2005.08.038

Barrett, E.F., and C.F. Stevens. 1972. The kinetics of transmitter release at the frog neuromuscular junction. *J. Physiol.* 227:691–708. https://doi.org/10.1113/jphysiol.1972.sp010054

Bouhours, B., F.F. Trigo, and A. Marty. 2011. Somatic depolarization enhances GABA release in cerebellar interneurons via a calcium/protein kinase C pathway. *J. Neurosci.* 31:5804–5815. https://doi.org/10.1523/JNEUROSCI.5127-10.2011

Chang, S., T. Trimbuch, and C. Rosenmund. 2018. Synaptotagmin-1 drives synchronous Ca^{2+}-triggered fusion by C_2B-domain-mediated synaptic-vesicle-membrane attachment. *Nat. Neurosci.* 21:33–40. https://doi.org/10.1038/s41593-017-0037-5

Christie, J.M., D.N. Chiu, and C.E. Jahr. 2011. $Ca^{(2+)}$-dependent enhancement of release by subthreshold somatic depolarization. *Nat. Neurosci.* 14:62–68. https://doi.org/10.1038/nn.2718

de San Martin, J.Z., A. Jalil, and F.F. Trigo. 2015. Impact of single-site axonal GABAergic synaptic events on cerebellar interneuron activity. *J. Gen. Physiol.* 146:477–493. https://doi.org/10.1085/jgp.201511506

Faas, G.C., K. Karacs, J.L. Vergara, and I. Mody. 2005. Kinetic properties of DM-nitrophen binding to calcium and magnesium. *Biophys. J.* 88:4421–4433. https://doi.org/10.1529/biophysj.104.057745

Forti, L., C. Pouzat, and I. Llano. 2000. Action potential-evoked Ca2+ signals and calcium channels in axons of developing rat cerebellar interneurones. *J. Physiol.* 527(Pt 1):33–48. https://doi.org/10.1111/j.1469-7793.2000.00033.x

Hallermann, S., and R.A. Silver. 2013. Sustaining rapid vesicular release at active zones: potential roles for vesicle tethering. *Trends Neurosci.* 36:185–194. https://doi.org/10.1016/j.tins.2012.10.001

Hallermann, S., C. Pawlu, P. Jonas, and M. Heckmann. 2003. A large pool of releasable vesicles in a cortical glutamatergic synapse. *Proc. Natl. Acad. Sci. USA.* 100:8975–8980. https://doi.org/10.1073/pnas.1432836100

Hallermann, S., A. Fejtova, H. Schmidt, A. Weyhersmüller, R.A. Silver, E.D. Gundelfinger, and J. Eilers. 2010. Bassoon speeds vesicle reloading at a central excitatory synapse. *Neuron.* 68:710–723. https://doi.org/10.1016/j.neuron.2010.10.026

Hosoi, N., T. Sakaba, and E. Neher. 2007. Quantitative analysis of calcium-dependent vesicle recruitment and its functional role at the calyx of Held synapse. *J. Neurosci.* 27:14286–14298. https://doi.org/10.1523/JNEUROSCI.4122-07.2007

Hosoi, N., M. Holt, and T. Sakaba. 2009. Calcium dependence of exo- and endocytotic coupling at a glutamatergic synapse. *Neuron.* 63:216–229. https://doi.org/10.1016/j.neuron.2009.06.010

Kaplan, J.H., and G.C. Ellis-Davies. 1988. Photolabile chelators for the rapid photorelease of divalent cations. *Proc. Natl. Acad. Sci. USA.* 85:6571–6575. https://doi.org/10.1073/pnas.85.17.6571

Kusick, G.F., M. Chin, K. Lippmann, K.P. Adula, W.M. Davis, E.M. Jorgensen, and S. Watanabe. 2018. Synaptic vesicles undock and then transiently dock after an action potential. *bioRxiv.* doi:. https://doi.org/10.1101/509216

Lee, J.S., W.K. Ho, and S.H. Lee. 2012. Actin-dependent rapid recruitment of reluctant synaptic vesicles into a fast-releasing vesicle pool. *Proc. Natl. Acad. Sci. USA.* 109:E765–E774. https://doi.org/10.1073/pnas.1114072109

Llinás, R., M. Sugimori, and R.B. Silver. 1992. Microdomains of high calcium concentration in a presynaptic terminal. *Science.* 256:677–679. https://doi.org/10.1126/science.1350109

Miki, T., G. Malagon, C. Pulido, I. Llano, E. Neher, and A. Marty. 2016. Actin- and myosin-dependent vesicle loading of presynaptic docking sites prior to exocytosis. *Neuron.* 91:808–823. https://doi.org/10.1016/j.neuron.2016.07.033

Miki, T., Y. Nakamura, G. Malagon, E. Neher, and A. Marty. 2018. Two-component latency distributions indicate two-step vesicular release at simple glutamatergic synapses. *Nat. Commun.* 9:3943. https://doi.org/10.1038/s41467-018-06336-5

Neher, E., and N. Brose. 2018. Dynamically primed synapic vesicle states: key to understand synaptic short-term plasticity. *Neuron.* 100:1283–1291. https://doi.org/10.1016/j.neuron.2018.11.024

Neher, E., and T. Sakaba. 2008. Multiple roles of calcium ions in the regulation of neurotransmitter release. *Neuron.* 59:861–872. https://doi.org/10.1016/j.neuron.2008.08.019

Nusser, Z., S. Cull-Candy, and M. Farrant. 1997. Differences in synaptic GABA(A) receptor number underlie variation in GABA mini amplitude. *Neuron.* 19:697–709. https://doi.org/10.1016/S0896-6273(00)80382-7

Pulido, C., and A. Marty. 2017. Quantal fluctuations in central mammalian synapses: Functional role of vesicular docking sites. *Physiol. Rev.* 97:1403–1430. https://doi.org/10.1152/physrev.00032.2016

Pulido, C., and A. Marty. 2018. A two-step docking site model predicting different short-term synaptic plasticity patterns. *J. Gen. Physiol.* 150:1107–1124. https://doi.org/10.1085/jgp.201812072

Pulido, C., F.F. Trigo, I. Llano, and A. Marty. 2015. Vesicular release statistics and unitary postsynaptic current at single GABAergic synapses. *Neuron.* 85:159–172. https://doi.org/10.1016/j.neuron.2014.12.006

Rossi, B., G. Maton, and T. Collin. 2008. Calcium-permeable presynaptic AMPA receptors in cerebellar molecular layer interneurones. *J. Physiol.* 586:5129–5145. https://doi.org/10.1113/jphysiol.2008.159921

Rossi, B., D. Ogden, I. Llano, Y.P. Tan, A. Marty, and T. Collin. 2012. Current and calcium responses to local activation of axonal NMDA receptors in developing cerebellar molecular layer interneurons. *PLoS One.* 7:e39983. https://doi.org/10.1371/journal.pone.0039983

Sakaba, T. 2006. Roles of the fast-releasing and the slowly releasing vesicles in synaptic transmission at the calyx of Held. *J. Neurosci.* 26:5863–5871. https://doi.org/10.1523/JNEUROSCI.0182-06.2006

Sakaba, T. 2008. Two $Ca^{(2+)}$-dependent steps controlling synaptic vesicle fusion and replenishment at the cerebellar basket cell terminal. *Neuron.* 57:406–419. https://doi.org/10.1016/j.neuron.2007.11.029

Sakaba, T., and E. Neher. 2001. Quantitative relationship between transmitter release and calcium current at the calyx of held synapse. *J. Neurosci.* 21:462–476. https://doi.org/10.1523/JNEUROSCI.21-02-00462.2001

Schneggenburger, R., and E. Neher. 2000. Intracellular calcium dependence of transmitter release rates at a fast central synapse. *Nature.* 406:889–893. https://doi.org/10.1038/35022702

Südhof, T.C. 2012. The presynaptic active zone. *Neuron.* 75:11–25. https://doi.org/10.1016/j.neuron.2012.06.012

Trigo, F.F., M. Chat, and A. Marty. 2007. Enhancement of GABA release through endogenous activation of axonal $GABA_A$ receptors in juvenile cerebellum. *J. Neurosci.* 27:12452–12463. https://doi.org/10.1523/JNEUROSCI.3413-07.2007

Trigo, F.F., T. Sakaba, D. Ogden, and A. Marty. 2012. Readily releasable pool of synaptic vesicles measured at single synaptic contacts. *Proc. Natl. Acad. Sci. USA.* 109:18138–18143. https://doi.org/10.1073/pnas.1209798109

Turecek, R., and L.O. Trussell. 2002. Reciprocal developmental regulation of presynaptic ionotropic receptors. *Proc. Natl. Acad. Sci. USA.* 99:13884–13889. https://doi.org/10.1073/pnas.212419699

Vere-Jones, D. 1966. Simple stochastic models for the release of quanta of transmission from a nerve terminal. *Aust. J. Stat.* 8:53–63. https://doi.org/10.1111/j.1467-842X.1966.tb00164.x

Wadel, K., E. Neher, and T. Sakaba. 2007. The coupling between synaptic vesicles and Ca2+ channels determines fast neurotransmitter release. *Neuron.* 53:563–575. https://doi.org/10.1016/j.neuron.2007.01.021

Wölfel, M., X. Lou, and R. Schneggenburger. 2007. A mechanism intrinsic to the vesicle fusion machinery determines fast and slow transmitter release at a large CNS synapse. *J. Neurosci.* 27:3198–3210. https://doi.org/10.1523/JNEUROSCI.4471-06.2007

Zorrilla de San Martín, J., F.F. Trigo, and S.-Y. Kawaguchi. 2017. Axonal $GABA_A$ receptors depolarize presynaptic terminals and facilitate transmitter release in cerebellar Purkinje cells. *J. Physiol.* 595:7477–7493. https://doi.org/10.1113/JP275369

Supplemental material

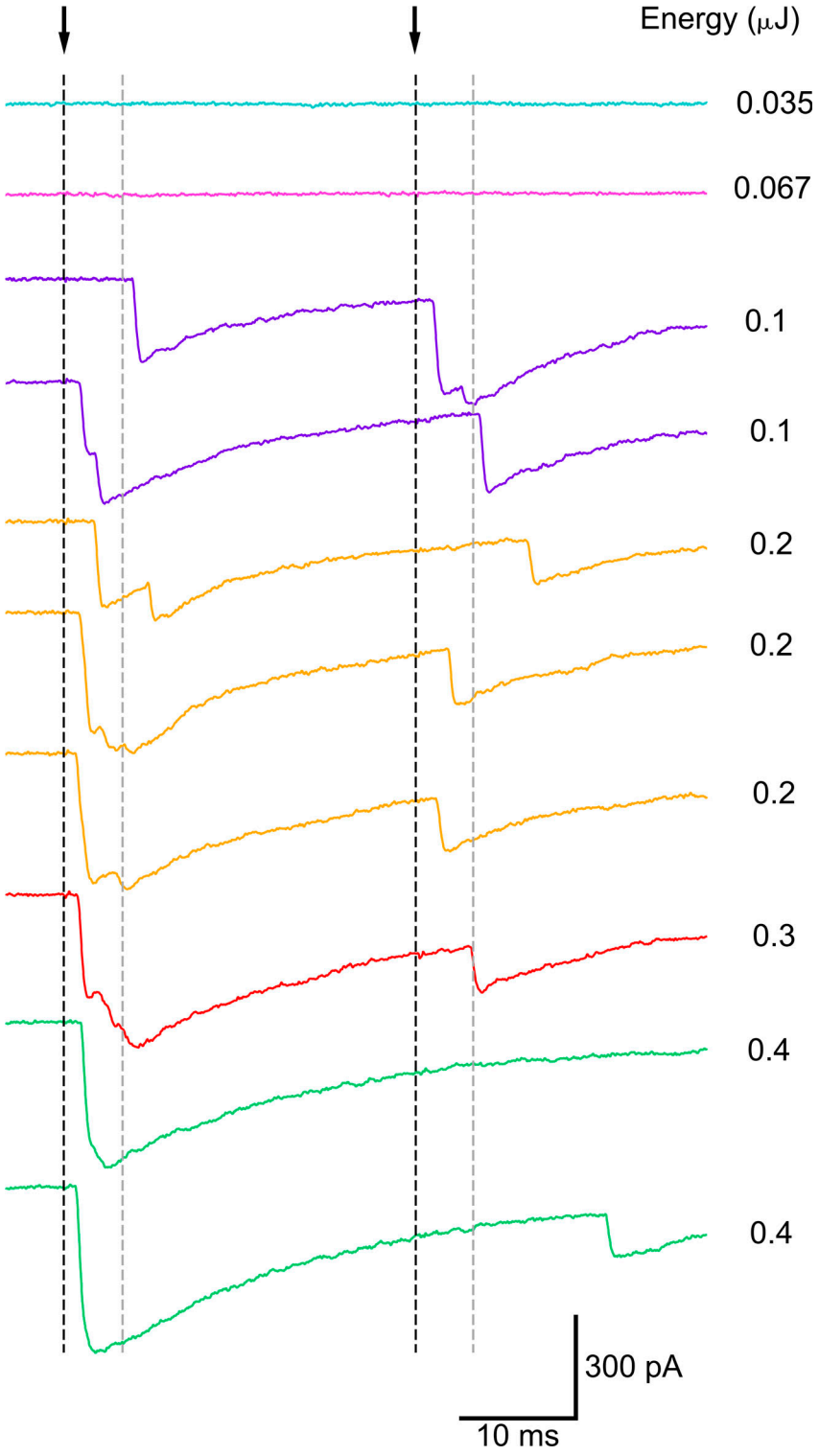

Figure S1. **Simple synapse response to double laser stimulation with increasing intensities.** Having established a simple synapse recording, two laser pulses were applied to the presynaptic varicosity, with 30-ms intervals between stimulations (arrows) and 1-min waiting times between pairs of stimulations. In conformity with previous observations (Trigo et al., 2012), when increasing the laser energy, initially only failures were obtained, and then multivesicular release responses were obtained with latencies that decreased as a function of laser intensity. Note that for laser intensities of 0.3 or 0.4 µJ, no response was recorded within 5 ms following the second laser stimulation (between black and gray vertical lines). Recording conditions for the second part of this work (Figs. 4 and 5) correspond to laser intensities of 0.3 or 0.4 µJ in this example; first latencies are then close to 2 ms. Recording conditions for the first part of this work (Figs. 1, 2, and 3) correspond to slightly larger laser intensities, with first latencies on the order of 1 ms.

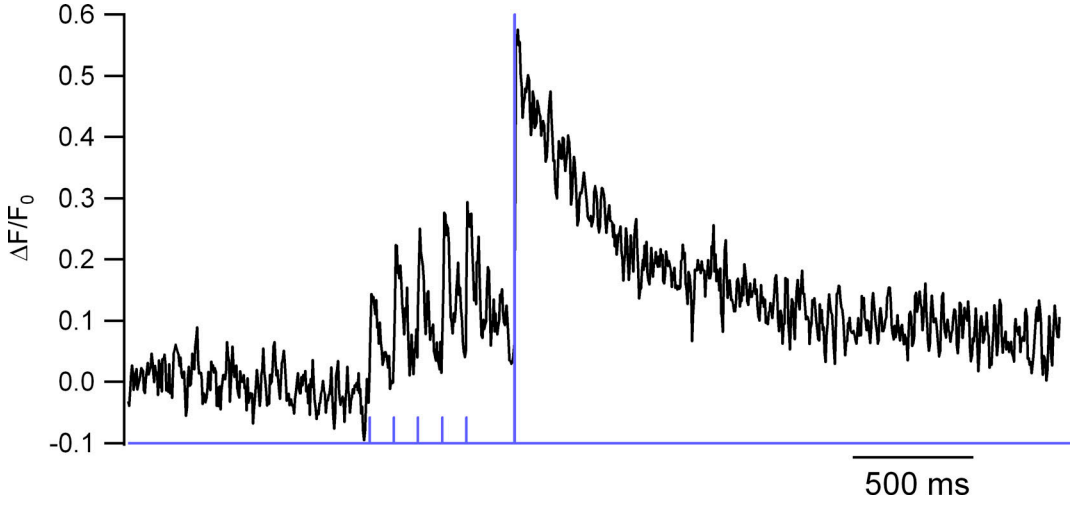

Figure S2. **Calcium response to conditioning laser pulses in a presynaptic terminal as measured with the high-affinity dye OGB1.** In this experiment, a presynaptic terminal was dialyzed with the high-affinity dye OGB1 (100 µM). A series of five laser pulses with small amplitude preceded a test laser pulse with large amplitude (blue trace). As illustrated in this recording, the peak OGB1 signal following the fifth prepulse is approximately half the peak amplitude recorded in response to the test pulse (mean ratio ± SD between these two amplitudes, 0.5 ± 0.09; n = 3 experiments). As the peak amplitude in response to the test pulse presumably reflects the maximum response of the dye, while the basal calcium concentration is negligible, this indicates that the peak amplitude following the fifth prepulse is close to the K_d of the dye, namely 170 nM.